Optimal placement of multiple morphogen sources

Y. Morishita[1,2] and Y. Iwasa[2]
[1]*PRESTO, Japan Science and Technology Agency, 4-1-8 Honcho Kawaguchi, Saitama, Japan*
[2]*Department of Biology, Faculty of Sciences, Kyushu University, Fukuoka 812-8581, Japan*
(Received 9 November 2007; published 16 April 2008)

During development, cells grow, differentiate, divide, and die according to their spatial positions, yet the positional information given to cells by morphogens (diffusive chemicals) includes considerable noises from various origins. In this paper, we examine a relationship between fluctuations in morphogen concentrations that the cells receive and the precision of positional specification by the morphogens in multidimensional space. As a method to quantify the precision, we introduce a measure of "ambiguity of positional information," based on the information entropy. We discover that the location of morphogen sources crucially affects the ambiguity, and that the ambiguity becomes minimum when the angle made by gradient vectors of different morphogens cross at a right angle in a target region under a given organ geometry (orthogonality principle). We conjecture that morphogen sources in development might be placed at the nearly optimal position that minimizes the ambiguity of positional information. This is supported by experimental data on the configurations of two major sources of spatial patterning, the apical ectodermal ridge (AER) and the zone of polarizing activity (ZPA), in vertebrate limb development. Indeed, their predicted configuration agrees very well with the one observed in experiments. We believe that the placement of morphogen sources to minimize the ambiguity of positional information is a basic principle in development of multicellular organisms beyond this particular example.

DOI: 10.1103/PhysRevE.77.041909 PACS number(s): 82.39.−k, 05.40.−a, 87.18.−h, 87.15.Ya

I. INTRODUCTION

To achieve normal development, cells need to differentiate, divide, grow, and die at proper timing and at proper locations. During morphogenesis of multicellular organisms, concentration gradients of diffusive chemicals, called morphogens, provide positional information to cells [1]. The morphogen concentrations involve noise originating from different sources such as embryo-to-embryo variability [2,3] and stochasticity in biochemical processes within each embryo [4–6]. The noise makes the positional information ambiguous. Nevertheless, the development of multicellular organisms is highly robust and reproducible. Thus the developmental process is likely to be designed to perform precise positional specification of cells despite the presence of noise. Some studies have proposed mechanisms to prevent the noise from propagating to downstream of signaling pathways and to reduce the noise itself [7–13]. Most of these focused on one-dimensional positional specification, e.g., along the anterior-posterior axis.

However, actual developmental processes occur in multidimensional space, where spatial positions are specified by multiple morphogens [14]. A crucial difference between positional specification in one-dimensional space and in multiple-dimensional space is the degree of freedom for the placement of morphogen sources. In many cases morphogen sources are localized on the boundary of organs [14]. In one-dimensional space, the boundary is composed of two points only, e.g., anterior and posterior poles. In contrast, in multidimensional space, the boundary is continuous and infinite combinations of the placement of morphogen sources are possible. Then, how is the configuration of morphogen sources determined in each developmental process?

Here we address the question of how to determine the location of morphogen sources. We first show that in two-dimensional space the geometrical configuration of multiple morphogen sources strongly affects the precision of positional information in the presence of noise. We then propose a general method to quantify the precision of positional information—we introduce two quantities, "local ambiguity" and "global ambiguity" of positional information based on the information entropy [15]. By using these measures, we find that the optimal configuration that gives the most precise positional information is achieved when the gradient vectors of different morphogen concentrations cross each other close to right angle in the target region such as the area of undifferentiated cells (i.e., orthogonality principle). We then examine usefulness of this idea by using an example of vertebrate limb development. We focus on the relative configuration of two sources of spatial patterning, the apical ectodermal ridge (AER) and the zone of polarizing activity (ZPA) [16–18]. We observe that their optimal configuration predicted by our theory agrees very well with that observed in experiments. The result supports a "minimum ambiguity hypothesis" which postulates that morphogen sources are placed in a manner to minimize the ambiguity of positional information in a target region under a given organ geometry.

II. MODEL AND METHOD

A. Basic ideas

We first illustrate our basic ideas with a simple example. Let us consider two morphogen gradients in the two-dimensional space (Fig. 1). In this paper, we use the word "morphogen" in a broad sense as any diffusive chemicals that have spatial distributions of their concentrations and affect spatial patterning (not necessarily cause direct induction of differentiation). A cell located at (x,y) in the real space receives a pair of morphogen concentrations (concentration

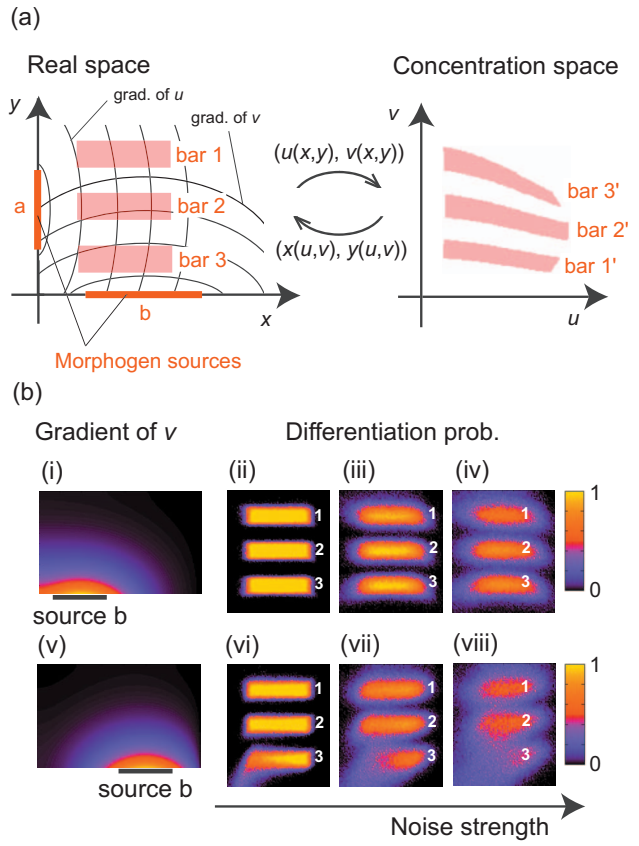

FIG. 1. (Color) Basic ideas of this study. (a) Relationship between real space (x-y plane) and concentration space (u-v plane). From the morphogen sources a and b, double gradients are formed. Each spatial point (x,y) corresponds to a specific point (u,v) in the concentration space. The pattern of three bars in the real space are mapped to the corresponding region, bar 1′, bar 2′, and bar 3′, in the concentration space. The u-v plane is represented in a log-log scale. (b) The precision of positional specification by morphogen gradients depends on the locations of morphogen sources as well as the magnitude of noise in morphogen concentrations sensed by cells. The left two figures (i) and (v) show the spatial pattern of concentration v with different locations of the source b. The location of the source a and the spatial pattern of u is the same in both cases (not shown). Figures (ii)–(iv) show the differentiation probability of the target bar structure, where the location of the source b is given in (i). Figures (vi)–(viii) is for the source location given in (v). Noise strength increases from the left to the right.

coordinate), $u(x,y)$ and $v(x,y)$. We assume that cells do not have additional information on their spatial positions (x,y) other than the morphogen concentrations. Spatial coordinates $(x(u,v),y(u,v))$ can be known once the morphogen concentrations (u,v) are given, thus we may regard $(x(u,v),y(u,v))$ as "positional information" in a mathematical sense.

Consider the case in which a spatial pattern is generated after cell differentiation based on the concentrations of two morphogens, as shown in Fig. 1(a). In this example, the target pattern consists of three bars in the real space. This pattern is mapped by $(u(x,y),v(x,y))$ to a region in the concentration space [bar 1′–bar 3′ in Fig. 1(a)]. Suppose that cells differentiate if and only if the concentrations (u,v) they experience are within the given region of the concentration space. If there is no noise in morphogen concentrations then the tissues are able to precisely develop the target pattern in the real space. However, in the presence of noise, e.g., fluctuations in the expression levels of morphogens at their sources and noises during the diffusion process, their concentrations sensed by each cell are modified and the differentiation pattern of the three bars to be produced in the real space becomes deformed and fuzzy [Fig. 1(b)]. When the magnitude of noise is large, the differentiation pattern is altered completely [Fig. 1(b)].

More importantly, for any given degree of noise, the fuzziness of the differentiation pattern to develop strongly depends on the location of the morphogen sources. For example, in the lower part in Fig. 1(b), it is difficult to recognize the bar structure under strong noise—especially bar 3 is merged with bar 2. In contrast, in the upper part in Fig. 1(b), the differentiation patterns remain close to the original three bar structure despite the noise of the same magnitude. This example demonstrates that the locations of morphogen sources affect the vulnerability of the pattern to noise and indicates that the maximum robustness may be achieved by a specific location of the second morphogen source.

It should be noted that the determination of cell fates involves many processes such as intracellular complex crosstalk among signaling pathways and intercellular interaction. However, the problem on the configuration itself can be discussed separately from the mechanisms for the readout of gradients or intercellular interaction.

B. Quantification of precision of positional information

In order to quantitatively evaluate the precision of positional specification by the concentration of multiple morphogens we introduce the information entropy $H(x,y)$ for an analog information source [15] defined as follows:

$$H(x,y) = -\int\int p(x',y';x,y)\ln p(x',y';x,y)dx'dy', \quad (1)$$

where $p(x',y';x,y)$ is the probability density function for the positional information (x',y') given to the cell located at (x,y). The stochasticity of the positional information is caused by the noise in the morphogen concentrations sensed by the cell. A larger $H(x,y)$ indicates a greater ambiguity in specifying spatial positions. $H(x,y)$ is defined for each spatial point (x,y). We call $H(x,y)$ the "local ambiguity" of positional information. In contrast, the ambiguity for a given spatial region Ω can be evaluated by the average of the local ambiguity $H(x,y)$ over the region

$$\Psi \equiv \frac{1}{|\Omega|}\int\int_{\Omega} H(x,y)dxdy, \quad (2)$$

where $|\Omega|$ is the area of Ω. We call Ψ the "global ambiguity" of positional information.

III. RESULTS

A. Determinants of precision of positional information

The local ambiguity $H(x,y)$ can be decomposed into three terms as follows (see Appendix A for the derivation):

$$H(x,y) = \ln \sqrt{\frac{\sigma_u{}^2\sigma_v{}^2 - C_{uv}^2}{(uv)^2}} + \ln \frac{2\pi e}{|\text{grad } u/u||\text{grad } v/v|} + \ln \frac{1}{|\sin \theta|}, \quad (3)$$

where $\text{grad } u = (\partial u/\partial x, \partial u/\partial y)$ and $\text{grad } v = (\partial v/\partial x, \partial v/\partial y)$ are gradient vectors of the two morphogens, and θ is the angle between these two gradient vectors. $\sigma_u{}^2$, $\sigma_v{}^2$, and C_{uv} are the variances of two morphogens and the covariance between them.

The first term on the right-hand side is the ambiguity caused by the fluctuations in morphogen concentrations. Naturally, this ambiguity becomes smaller with the decrease in the fluctuations. Provided that each standard deviation of morphogen concentration u and v is proportional to the corresponding average (e.g., in the case of environmental noise), this term is constant and independent of spatial position (x,y).

The second term of Eq. (3) is determined by $|\text{grad } u/u|$ and $|\text{grad } v/v|$. In the one-dimensional case, if the morphogen gradient c is given by $c = c_0 \exp(-ax)$ [2], then $|\text{grad } c/c|$ is equal to the exponent a. When the gradient is formed by simple diffusion and linear degradation, the value of a corresponds to the ratio of the degradation rate to the diffusion coefficient of the chemical. In the two-dimensional case, the values of $|\text{grad } u/u|$ and $|\text{grad } v/v|$ are mainly controlled by the ratio, although they also depend on the shapes of the boundary or the morphogen sources. Thus, the second term of Eq. (3) can be interpreted as the ambiguity determined by physical properties of the two morphogens, and the value of the term is almost independent of spatial position (x,y). The magnitude of this term decreases with the increase in the steepness of the gradients. It should be noted that the above discussion holds even if the gradient is formed by other mechanisms than simple diffusion [19–25] as long as the gradient can be approximated by an exponential curve.

The above two terms are involved in the positional specifications both in one-dimensional space and in multidimensional space [see Eq. (A5) in Appendix A]. In contrast, the last term in Eq. (3) appears only in the multidimensional case. The term is the ambiguity determined by the angle between the two gradient vectors $\text{grad } u$ and $\text{grad } v$ and it reflects geometric information of organs. The value of this term changes most clearly according to the spatial position (x,y). Further, among the three terms contributing the local ambiguity $H(x,y)$, the third term is the most strongly affected by the locations of two morphogen sources and has the largest impact on the robustness of the positional specification. At each local position, it is minimized when the gradient vectors cross at a right angle.

On the other hand, it is not possible to make the angle perfectly orthogonal everywhere in a given region Ω. Therefore, it is important to examine how the global ambiguity Ψ [Eq. (2)] changes with the configuration of morphogen sources in a given organ geometry.

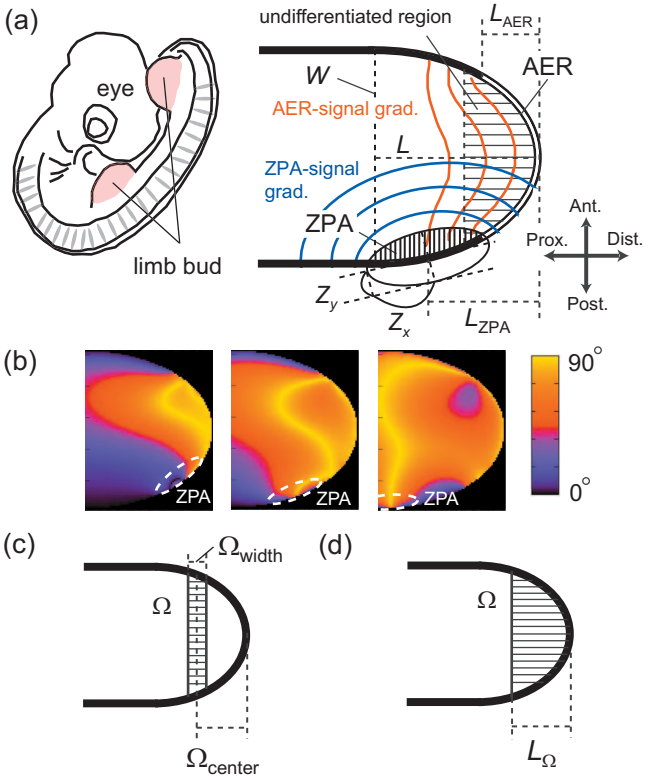

FIG. 2. (Color) Application of our theory to vertebrate limb development. (a) A simple scheme for a limb bud. Limb bud shape is modeled as an extended semiellipsoid (see Appendix B for details). The red and blue lines show concentration contours of the AER signal and ZPA signal, respectively. The shaded area at the tip of the limb bud is the undifferentiated region. (b) Distributions of angle made by two gradient vectors for the AER signal and ZPA signal. The angle distribution is strongly affected by the location of ZPA. (c),(d) Two possible choices on where to be given precise positional information, Ω in the global ambiguity Ψ. Case 1 (c): cells in the undifferentiated region require precise information on their positions to determine their fates only when they are pushed out of the region as a result of limb outgrowth, that is, only when they are around the boundary of the undifferentiated region. Ω is characterized by the center of the band Ω_{center} and its width Ω_{width}. Case 2 (d): All cells in the undifferentiated region require precise positional information whether they are near the boundary or not. Ω is characterized by the distance of the boundary of the undifferentiated region from the tip L_Ω.

B. Biological application: Configuration of AER and ZPA in vertebrate limb development

1. Biological background

As a possible example of our analysis, we consider the configuration of the zone of polarizing activity (ZPA) and apical ectodermal ridge (AER), which are major sources of spatial patterning in vertebrate limb development [16,17]. The ZPA is a mesodermal region localized at the posterior margin in the limb bud (Fig. 2). It is responsible for normal antero-posterior (*A-P*) patterning including cartilage and digit formation. When the ZPA is removed by surgery in early limb bud formation, the digit pattern is lost and limbs continue to extend [26]. Its graft to the anterior leads to a

mirror image of the posterior limb [27]. The gradient of the Sonic hedgehog protein (SHH) secreted from the ZPA is believed to give the positional information along the *A-P* axis [28–34].

The patterning mechanism along the *P-D* axis is not settled. The classical hypothesis for the *P-D* specification is called the "progress zone model" [35,36], which postulates that the history of environment experienced by each cell (the stay duration in the progress zone) plays an important role. In contrast, in an alternative model called the "early specification model" [36,37], the cell fate along the *P-D* axis is already determined in early stages of development. However, according to the most recent paper by Tabin and Wolpert [16], neither of these fits the recent findings of molecular biology; rather, the *P-D* patterning is now considered to be formed through dynamic changes of gene expression patterns during the outgrowth of a limb.

At the present time, fibroblast growth factors (FGFs) from the AER (a thickening in the ectoderm at the tip of the limb bud) are believed to play an important role for the formation of an apical undifferentiated region through the inhibition of differentiation and/or apoptosis of mesenchymal cells [16]. Based on experiments, the undifferentiated region ranges about 200 μm–300 μm from the tip. The range is considered to be determined by the concentration of FGFs (in the following analysis, it is not a problem whether the determination is done in an all-or-none manner or in a graded manner).

The fates of cells in the undifferentiated region are not determined in contrast to those in the proximal region with determined fates. In addition, from studies on the fate map [38,39], the movement and the change of relative position of cells in the proximal region are smaller compared to those in the undifferentiated region. Therefore, it is quite plausible to assume that precise positional information is much more important for cells in the undifferentiated region than those in the proximal region.

In the following, we discuss the optimal position of the ZPA [L_{ZPA} in Fig. 2(a)] that gives the most precise positional information to the undifferentiated cells in two-dimensional (2D) space spanned by the *A-P* and *P-D* axes. Actually, as shown later, the distance between the AER and the ZPA is kept almost constant during the outgrowth. We ask how the distance affects the precision of positional information and what configuration achieves the most accurate positional specification of mesenchymal cells at each time point of development. We examined two cases differing on where to be given precise positional information [see Fig. 2(c) and 2(d)]. In case 1, cells in the undifferentiated region require precise information on their positions to determine their fates only when they are pushed out of the region as a result of limb outgrowth, that is, only when they are around the boundary of the undifferentiated region (e.g., 200 μm–300 μm). In case 2, all cells in the undifferentiated region require precise positional information whether they are near the boundary or not. Actually, as shown later, an optimal position of the ZPA is the same between two cases. Thus, our interest here is not to discuss which of the two choices is more appropriate, but the existence of the optimal position of the ZPA from the viewpoint of robustness against noise. We show later that the optimal position is consistent with the experimentally observed one.

In the following, we regard the AER and ZPA as sources of primary positional information in 2D space as discussed before; they release signals to determine the range of the undifferentiated region and the positional value along the *A-P* axis, respectively. We will refer to the AER-derived *P-D* signal and ZPA-derived *A-P* signal as the "AER signal" and "ZPA signal," respectively, and not refer to concrete substances of these signals although their major candidates are FGFs and SHH, respectively.

It should be noted that we do not mean that the signals from the AER and the ZPA necessarily specify cell fates or change their behavior immediately. Instead, these signals might affect cell fate and their behavior which will appear in much later stages through complex crosstalk among multiple signaling pathways. As stated before, we can discuss the effect of the configuration of morphogen sources on the robustness of spatial patterning separately from the complex intracellular mechanisms for the readout of signals, such as FGFs and SHH, although the latter is also an important problem in developmental biology.

2. Analysis

As explained above, we considered the AER and ZPA as sources of two-dimensional positional information to undifferentiated regions in vertebrate limb development, and applied our theory for the optimal placement of morphogen sources. Then we compared the theoretically derived optimal configuration of these sources with the configuration reported for the real developmental processes of chicks and mice.

We approximated the shape of the limb bud tip as a semiellipsoid, which holds fairly well for stages up to E11.0 for mice and stages up to 24 for chicks [see Fig. 2(a)]. In the following, spatial scales, such as the size of morphogen sources and the distance between sources, are expressed as values relative to the limb bud width W [see Fig. 2(a) and Appendix B for the details of modeling]. The spatial distribution of the AER signal and ZPA signal were formed by simple diffusion with linear degradation of molecules [see Eq. (B1)]. We used the two-dimensional model for the limb bud although the real limb bud has a three-dimensional shape. This is because the protein WNT that can be regarded as a source for positional information along the dorso-ventral (*D-V*) axis is expressed widely in the dorsal region. Hence we can assume that the gradient along the *D-V* axis is almost orthogonal to the plane spanned by the *A-P* and the *P-D* axes.

As shown in Fig. 2(b), the spatial distribution of the angle made by the gradient vectors for the AER signal and ZPA signal drastically changed with the position of the ZPA. It is not possible to make the angle of two gradient vectors perfectly orthogonal everywhere on the limb bud. Therefore, we searched for the condition that minimized the global ambiguity of positional information Ψ given in Eq. (2). We examined two cases that differ in the region Ω to be integrated in Eq. (2) (see Sec. III B 1). In case 1, Ω was chosen as the area around the boundary of the undifferentiated region

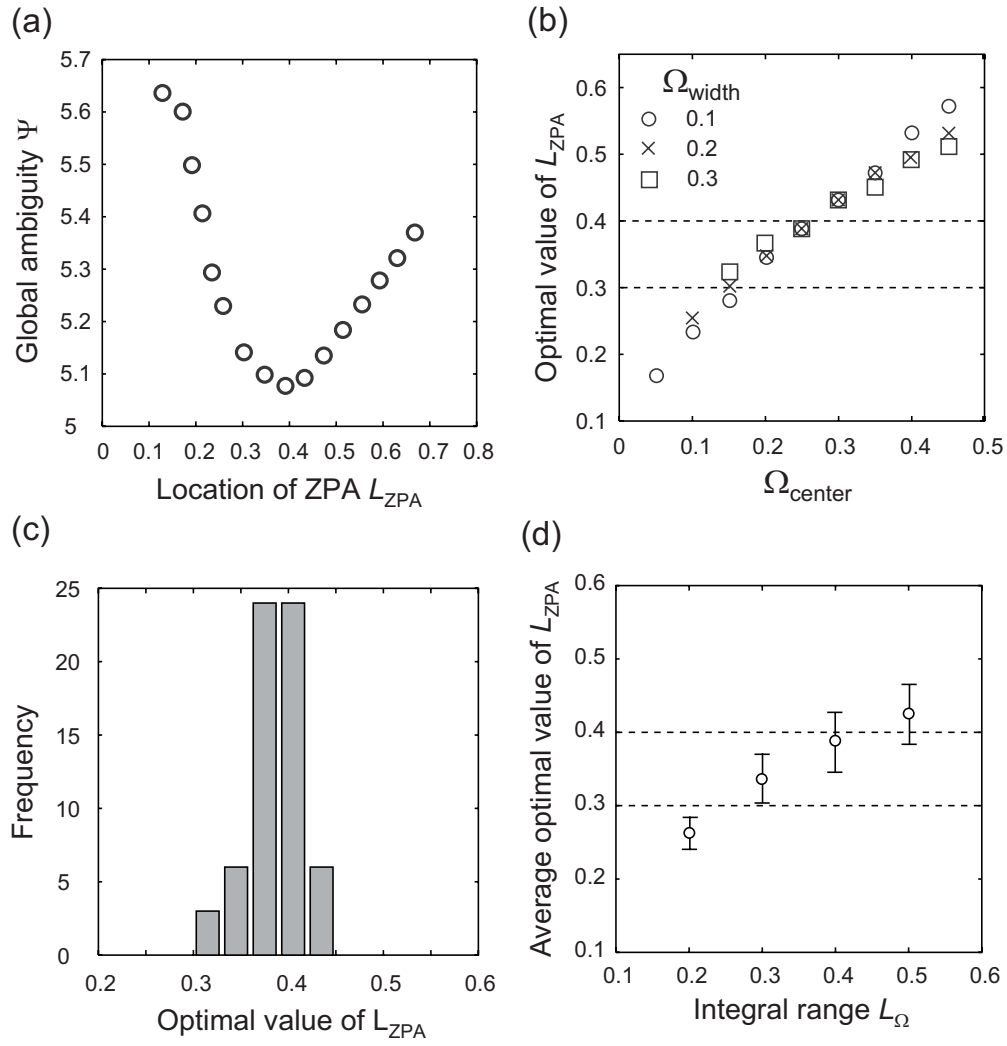

FIG. 3. Optimal condition for the ZPA position to minimize the global ambiguity Ψ. (a) The optimal location of the ZPA that minimizes the ambiguity of positional information is around $L_{ZPA}=0.35-0.4$, which agrees well with the experimentally observed values (see Table I). The horizontal and vertical axes indicate the location of ZPA L_{ZPA} and the global ambiguity Ψ, respectively. Parameters: $(L, L_{AER}, Z_x, Z_y, \Omega_{center}, \Omega_{width})=(0.8, 0.25, 0.2, 0.1, 0.25, 0.1)$. (b) The optimal value of L_{ZPA} hardly depends on the area of Ω (i.e., Ω_{width}), but depends on the position of Ω (i.e., Ω_{center}), suggesting that the position of the information source (ZPA) is closely related to the region where precise positional information has to be given. Parameters other than Ω_{center} and Ω_{width} are the same as those in (a). (c) Histogram of the optimal value of L_{ZPA} over 63 different parameter sets: L (0.6–0.8 step 0.1), L_{AER} (0.15–0.45 step 0.05), Z_x (0.15–0.25 step 0.05). The optimal value is robust for parameter changes. Ω_{center} and Ω_{width} are set to be 0.25 and 0.1, respectively. (d) The average optimal distance for L_{ZPA}. The horizontal axis is the size of the undifferentiated region L_Ω. For each L_Ω, the average is calculated over the same 63 different parameter sets as those in Fig. 3(c). Error bars show one standard deviation from the average. From experimental observation, the value of L_Ω is estimated as nearly 0.3. For this range of L_Ω, the optimal distance of L_{ZPA} was predicted to be around 0.3–0.4, which is fairly consistent with the actual location of the ZPA.

[Fig. 2(c)]. Concretely, it was set to be a band with the width Ω_{width} and the center from the tip Ω_{center}. Based on experimental studies [35], we set Ω to range from 200 μm–300 μm from the tip, which corresponds to $\Omega_{width}=0.1$ and $\Omega_{center}=0.25$ in the model. On the other hand, in case 2, Ω was set to be the whole of the undifferentiated region and it is characterized by the distance of the boundary of the region from the tip, L_Ω [Fig. 2(d)]. We set $L_\Omega=0.3$. As stated before, both cases lead to similar results of the optimal placement of the ZPA. In the following analysis, we first focus on case 1 and discuss case 2 later.

Figure 3(a) shows the relation between the global ambiguity Ψ and the ZPA distance L_{ZPA}, for realistic parameter values. The U-shape curve clearly shows that there exists an optimal distance of the ZPA from the tip to achieve the most precise positional specification by the AER signal and ZPA signal. As shown in Fig. 2(b), when the ZPA is too close to the tip, the intersection of the two gradient vectors deviates from a right angle in a wide area. If the sources of two signals are too close to each other, their gradient vectors have a similar direction. In contrast, when the ZPA is distant from the tip, the gradient vectors are not close to orthogonal near the tip, although they may be close to orthogonal for cells in the proximal region that have already been differentiated.

TABLE I. Distance between the limb bud tip and the center of the *Shh* gene expression region.

Species	Limb[a]	Stage	L_{ZPA}[b]	Ref.
Chick	FL	st. 20	0.34	[40]
Chick	FL	st. 23	0.4	[28]
Chick	FL	st. 23	0.3	[41]
Chick	FL	st. 24	0.3	[42]
Mouse	FL	E9.5	0.38	[43]
Mouse	FL	E10.0	0.38	[43]
Mouse	FL	E10.5	0.37	[44]
Mouse	FL	E10.5	0.4	[45]
Mouse	FL	E11.0	0.4	[46]
Mouse	HL	E11.0	0.34	[46]

[a]FL and HL indicate forelimb and hindlimb, respectively.
[b]The values are normalized by limb width.

Figure 3(a) shows that the optimal value of L_{ZPA} is around 0.35–0.4 times the width of the limb bud, W (see Fig. 2 for the definition of W). As shown in Fig. 3(b), the optimal value hardly depends on the area of Ω (i.e., Ω_{width}), but depends on the position of Ω (i.e., Ω_{center}). This suggests that the position of the information source (ZPA) is closely related to the region where precise positional information has to be given.

Furthermore, the optimal distance does not change much when parameters such as the limb bud shape and the source sizes of the AER and ZPA are modified. Figure 3(c) shows the histogram of the optimal value of L_{ZPA} over 63 different parameter sets which covers the parameter ranges that are biologically plausible. In most cases, the value of L_{ZPA} is around 0.39. In addition, the optimal distance hardly changes even when the integral region is restricted to a somewhat posterior side, e.g., to around half of the limb width (data not shown).

To compare the optimal value of L_{ZPA} obtained by our theory with experimental observations, we measured the distance between the limb bud tip and the center of the *Shh* gene expression region (ZPA) in photographs of experimental papers for chicks and mice. As shown in Table I, in all cases, the value of L_{ZPA} were between 0.3 and 0.4, which is close to the optimal value to achieve the minimum ambiguity of positional information. This supports the idea that the source of the ZPA signal is in fact placed so as to achieve the most robust development.

On the other hand, when we adopted an alternative criterion in case 2 [see Fig. 2(d)], similar results such as a U-shape curve as shown in Fig. 3(a) were obtained (not shown). Figure 3(d) shows the average of optimal distance $\langle L_{ZPA} \rangle$ for different integral ranges L_Ω. For each L_Ω, the average was calculated over the same 63 different parameter sets as those used in Fig. 3(c). Error bars indicate one standard deviation from the average. The optimal distance changes with the range of region to be integrated L_Ω, suggesting that the ZPA position is closely related to the region where precise positional information has to be given as shown in case 1. The size of the undifferentiated region corresponds to about $L_\Omega = 0.3$ in our model, and the optimal distance of L_{ZPA} is around 0.3–0.4, which agrees well with the experimentally observed values shown in Table I.

To summarize the results of both cases, the position of the ZPA observed in real embryos is close to the optimal that provides precise positional information. This is so for both choices of the target region Ω. Although this analysis cannot conclude which of the two criteria for optimization is more appropriate, we can conclude that there exists the optimal location of the ZPA, which agrees well with the observed one.

IV. DISCUSSION

We have addressed how morphogen sources should be placed to achieve morphogenesis robust against noise, which is a problem specific to the multidimensional positional specification. To quantify the precision of positional information in a given region, we have introduced quantities, "ambiguity of positional information" H (local) and Ψ (global) based on the information entropy. We have clarified the origins of the local ambiguity: the magnitude of concentration noise, the gradient steepness, and the angle made by gradient vectors. The last one is the most strongly affected by the locations of morphogen sources and has the largest impact on the robustness of the positional specification. It is minimized when the gradient vectors cross at a right angle. This paper gives a clear and plausible argument for why this is so. We may call this concept the "orthogonal principle."

To illustrate the usefulness of our theory, we have considered the configuration of the two information sources, the AER and ZPA, in vertebrate limb development. As a result, we have observed the quantitative agreement between the theoretically derived optimal position of the ZPA and the experimentally observed one. We have also shown that the optimal position of the information source is closely related to the region where precise positional information has to be given. We believe that the idea of optimal placement of morphogen sources is useful in understanding many developmental processes other than vertebrate limb development.

All results in the present paper are calculated in the steady state. We think that the quasiequilibrium assumption is a proper one at least as a first step, in which the time scale of chemical dynamics is much faster than that of organ growth and deformation. It is a major challenge to examine how positional information is regulated in a nonstationary manner. In fact, developmental processes occur in a dynamically growing domain and morphogen concentrations at sources can change with time [54]. For example, Bergman *et al.* [47] suggested that decoding the pre-steady-state morphogen profile can reduce patterning errors.

We also found that the size of morphogen sources affects the precision of positional information although the effect is not as large as the effect of the location of morphogen sources (not shown). Further investigation will clarify the relation between the size of morphogen sources and the precision of positional specification.

Most of the previous experimental and theoretical studies on morphogens have focused on the mechanisms behind their formation and the interpretation of their gradients

[19–25,48–53]. Thus, the present study provides an insight into developmental biology, namely, how the configuration of morphogen sources or the expression patterns of diffusive chemicals should be arranged for robust morphogenesis. The present work supports a "minimum ambiguity hypothesis" which postulates that morphogen sources are located to minimize the global ambiguity of positional information Ψ in target regions.

ACKNOWLEDGMENTS

This work was done with the support of a Grant-in-Aid from JSPS. We thank the following people for their very helpful comments: B. Adams, K. Fujimoto, T. Gregor, S. Ishihara, K. Kaneko, T. Miura, B. Pfeuty, K. Sato, S. Sawai, and K. Tamura.

APPENDIX A: DERIVATION OF EQ. (3)

Let $\mathbf{c}=[u(x,y),v(x,y)]^T$ be the concentrations of two chemicals, given to a cell located at a spatial position $\mathbf{r}=(x,y)^T$, where T indicates transpose of the vector. Around each position $\mathbf{r}_0=(x_0,y_0)^T$, the following relation is satisfied as a first-order approximation:

$$\begin{pmatrix}\Delta u\\ \Delta v\end{pmatrix} \approx \begin{pmatrix}u_x & u_y\\ v_x & v_y\end{pmatrix}_{\mathbf{r}_0}\begin{pmatrix}\Delta x\\ \Delta y\end{pmatrix} \equiv G\begin{pmatrix}\Delta x\\ \Delta y\end{pmatrix}, \tag{A1}$$

where $\Delta\mathbf{r}\equiv(\Delta x,\Delta y)^T$ and $\Delta\mathbf{c}\equiv(\Delta u,\Delta v)^T$ are the deviation vectors of the position and of the morphogen concentration from $\mathbf{r}_0=(x_0,y_0)^T$ and $\mathbf{c}_0=(u_0,v_0)^T\equiv(u(x_0,y_0),v(x_0,y_0))$, respectively. Suffixes for u and v indicate partial derivatives such as $u_x\equiv\partial u/\partial x$. Thus, G is a linear map from a point around $\mathbf{r}_0$ in the real space to a point around $\mathbf{c}_0$ in the concentration space. With the inverse matrix, $F\equiv G^{-1}$, we have

$$\begin{pmatrix}\Delta x\\ \Delta y\end{pmatrix} = F\begin{pmatrix}\Delta u\\ \Delta v\end{pmatrix} = \frac{1}{|G|}\begin{pmatrix}v_y & -u_y\\ -v_x & u_x\end{pmatrix}_{\mathbf{r}_0}\begin{pmatrix}\Delta u\\ \Delta v\end{pmatrix}, \tag{A2}$$

where $|G|$ is the determinant of the matrix G.

Next, we consider the relationship between the fluctuations in the concentration space and those in the real space. Here we assume that fluctuations of two chemical concentrations obey a two-variable normal distribution with variance-covariance matrix Σ, which is added to the morphogen concentration sensed by cells. Then, the concentration fluctuations around $\mathbf{c}_0=(u_0,v_0)^T$ correspond to the fuzziness of positional specification around $\mathbf{r}_0=(x_0,y_0)^T$ in the real space characterized by the variance-covariance matrix Σ'. By using Eq. (A2), Σ' can be written as follows:

$$\Sigma' = F\Sigma F^T = \frac{1}{|G|^2}\begin{pmatrix}v_y & -u_y\\ -v_x & u_x\end{pmatrix}\begin{pmatrix}\sigma_u{}^2 & C_{uv}\\ C_{uv} & \sigma_v{}^2\end{pmatrix}\begin{pmatrix}v_y & -v_x\\ -u_y & u_x\end{pmatrix}, \tag{A3}$$

where $\sigma_u{}^2$ and $\sigma_v{}^2$ are the variances of concentrations u and v around $\mathbf{c}_0$, and C_{uv} is the covariance. For a two-variable normal distribution, the entropy $H(x,y)$ is given by

$$H(x,y) = \ln(2\pi e\sqrt{|\Sigma'|}). \tag{A4}$$

Substituting Eq. (A3) into Eq. (A4), Eq. (3) is obtained.

Geometrically, the origins of the three terms in Eq. (3) may be understood as follows. The area in the real space specified by $[u,u+du]\times[v,v+dv]$ is approximated by $dudv/|\text{grad } u||\text{grad } v||\sin\theta|$ when the fluctuations du and dv are small. $dudv/|\text{grad } u||\text{grad } v|$ corresponds to the first and the second terms in Eq. (3), and $1/|\sin\theta|$ corresponds to the third term.

In the one-dimensional case, the last term in Eq. (3) does not appear. From simple calculations, the ambiguity $H(x)$ becomes as follows:

$$H(x) = \ln\frac{\sigma_u}{u} + \ln\frac{\sqrt{2\pi e}}{|(du/dx)/u|}, \tag{A5}$$

where the first term is the ambiguity caused by the fluctuations in morphogen concentrations, and the second term is the ambiguity determined by the gradient steepness.

Similarly, we can easily extend the above calculations to the case of three-dimensional positional specification by three morphogens. Then, the entropy in Eq. (A4) becomes as follows:

$$H(x,y,z) = \frac{1}{2}\ln[(2\pi e)^3|\Sigma'|], \tag{A6}$$

where z is an additional dimension of the real space. Like the two-dimensional case, the local ambiguity $H(x,y,z)$ in the three-dimensional case can be decomposed into three terms as Eq. (3).

In this study, we consider the case in which the dimensions of the real space and of the concentration space are the same. If these are different, there is no one-to-one correspondence between the two spaces. In such a situation, we need additional assumptions to define a map from the concentration space to the real space, which is beyond the scope of this study [54].

APPENDIX B: MODELING OF LIMB BUD SHAPE AND MORPHOGEN GRADIENTS

We approximate the limb bud shape as a semiellipsoid with the width W in the antero-posterior direction and the length L in the proximo-distal direction [see Fig. 2(a)]. This approximation is fairly good for stages up to E11.0 for mice and stages up to 24 for chicks. The AER is defined as an arc within the distance L_{AER} from the tip of the limb bud. The ZPA is defined as an overlap region between the semiellipsoid for the limb bud and an ellipsoid with the center being on the posterior boundary of the limb bud. The distance between the ZPA center and the limb bud tip is designated by L_{ZPA}. The orientation of the ellipsoid is determined so that one principal axis is tangent to the semiellipsoid [see Fig. 2(a)], and the lengths of the principal axes are Z_x and Z_y. In the following, we set to $W=1$ and the other scales L, L_{AER}, L_{ZPA}, Z_x, and Z_y are expressed as relative values to the limb width W.

The diffusion and degradation processes of the AER signal u and the ZPA signal v in the mesenchymal tissue are written as the following equation:

$$\frac{\partial}{\partial t}C(x,y) = D\nabla^2 C(x,y) - \gamma C(x,y), \tag{B1}$$

where C is the concentration of two signals ($C=u$ or v), and D and γ are diffusion and degradation constants. At the ZPA (posterior mesenchyme), the ZPA signal is synthesized and released into the extracellular environment. To describe this, we added the source activity of the ZPA signal at the ZPA (a constant value) on the right-hand side of Eq. (B1). A zero-flux boundary condition is adopted. In contrast, the AER signal is synthesized at the ectodermal tissue which is located outside the mesenchymal tissue. We assume that the level of the AER signal at the boundary is constant, and that its value is determined by processes in the ectoderm.

The standard deviations of the ZPA signal and the AER signal are assumed to be proportional to their mean values (environmental noise). Since the undifferentiated region is close to their morphogen sources, we do not consider the alternative mode of noise in which the standard deviations are proportional to the square root of the means, which is important if the number of morphogen molecule is very small.

We calculated all results in the steady state, where production, decay, and diffusion are balanced. The optimal configuration for AER and ZPA obtained in this study hardly depends on parameters such as D, γ, or the source strengths.

[1] L. Wolpert, J. Theor. Biol. **25**, 1 (1969).
[2] B. Houchmandzadeh, E. Wieschaus, and S. Leibler, Nature (London) **415**, 798 (2002).
[3] T. Gregor, D. W. Tank, E. F. Wieschaus, and W. Bialek, Cell **130**, 153 (2007).
[4] J. Paulsson, Nature (London) **427**, 416 (2004).
[5] Y. Morishita, T. J. Kobayashi, and K. Aihara, J. Theor. Biol. **235**, 241 (2005).
[6] Y. Morishita, T. J. Kobayashi, and K. Aihara, Biophys. J. **91**, 2072 (2006).
[7] A. Eldar, R. Dorfman, D. Weiss, H. Ashe, B.-Z. Shilo, and N. Barkai, Nature (London) **419**, 304 (2002).
[8] A. Eldar, D. Rosin, B-Z. Shilo, and N. Barkai, Dev. Cell **5**, 635 (2003).
[9] B. Houchmandzadeh, E. Wieschaus, and S. Leibler, Phys. Rev. E **72**, 061920 (2005).
[10] T. Bollenbach, K. Kruse, P. Pantazis, M. Gonzalez-Gaitan, and F. Julicher, Phys. Rev. Lett. **94**, 018103 (2005).
[11] M. Howard and P. Reinten Wolde, Phys. Rev. Lett. **95**, 208103 (2005).
[12] T. Aegerter-Wilmsen, C. M. Aegerter, and T. Bisseling, J. Theor. Biol. **234**, 13 (2005).
[13] H. L. Ashe and J. Briscoe, Development **133**, 385 (2006).
[14] S. Gilbert, *Developmental Biology*, 8th ed. (Sinauer Associates, Sunderland, MA, 2006).
[15] C. E. Shannon and W. A. Weaver, *Mathematical Theory of Communication* (University of Illinois Press, Chicago, 1963).
[16] C. Tabin and L. Wolpert, Genes Dev. **21**, 1433 (2007).
[17] C. Tickle, Nat. Rev. Mol. Cell Biol. **7**, 45 (2006).
[18] T. Hirashima, Y. Iwasa, and Y. Morishita, Bull. Math. Biol. **70**, 438 (2008).
[19] A. A. Teleman, M. Strigini, and S. M. Cohen, Cell **105**, 559 (2001).
[20] A. A. Teleman and S. M. Cohen, Cell **103**, 971 (2000).
[21] M. Strigini and S. M. Cohen, Curr. Biol. **10**, 293 (2000).
[22] A. D. Lander, Q. Nie, and F. Y. M. Wan, Dev. Cell **2**, 785 (2002).
[23] M. Kerszberg and L. Wolpert, J. Theor. Biol. **191**, 103 (1998).
[24] T. B. Kornberg and A. Guha, Curr. Opin. Genet. Dev. **17**, 264 (2007).
[25] M Gonzalez-Gaitan, Nat. Rev. Mol. Cell Biol. **4**, 213 (2003).
[26] S. M. Pangan, M. A. Ros, C. Tabin, and J. F. Fallon, Dev. Biol. **180**, 35 (1996).
[27] J. W. Saunders, Jr. and M. T. Gasseling, *Epithelium—Mesenchymal Interaction* (Williams and Wilkins, Baltimore, MD, 1968).
[28] R. D. Riddle, R. L. Johnson, E. Laufer, and C. J. Tabin, Cell **75**, 1401 (1993).
[29] B. Wang, J. F. Fallon, and P. A. Beachy, Cell **100**, 423 (2000).
[30] C. Chiang, Y. Litingtung, M. P. Harris, B. K. Simandl, Y. Li, P. A. Beachy, and J. F. Fallon, Dev. Biol. **236**, 421 (2001).
[31] P. Kraus, D. Fraidenraich, and C. A. Loomis, Mech. Dev. **100**, 45 (2001).
[32] J. A. Goetz, L. M. Suber, X. Zeng, and D. J. Robbins, BioEssays **24**, 157 (2002).
[33] Y. Li, H. Zhang, Y. Litingtung, and C. Chiang, Proc. Natl. Acad. Sci. U.S.A. **103**, 6548 (2006).
[34] E. McGlinn and C. Tabin, Curr. Opin. Genet. Dev. **16**, 426 (2006).
[35] D. Summerbell, J. H. Lewis, and L. Wolpert, Nature (London) **244**, 492 (1973).
[36] M. Torres, J-P. Couso, and M. A. Ros, EMBO Rep. **3**, 933 (2002).
[37] A. T. Dudley, M. A. Ros, and C. J. Tabin, Nature (London) **418**, 539 (2002).
[38] N. Vargesson, J. D. W. Clarke, K. Vincent, C. Coles, L. Wolpert, and C. Tickle, Development **124**, 1909 (1997).
[39] K. Sato, Y. Koizumi, M. Takahashi, A. Kuroiwa, and K. Tamura, Development **134**, 1397 (2007).
[40] K. E. Lewis, G. Drossopoulou, I. R. Paton, D. R. Morrice, K. E. Robertson, D. W. Burt, P. W. Ingham, and C. Tickle, Development **126**, 2397 (1999).
[41] C. Rallis, B. G. Bruneau, J. D. Buono, C. E. Seidman, J. G. Seidman, S. Nissim, C. J. Tabin, and M. P. O. Logan, Development **130**, 2741 (2003).
[42] J. J. Sanz-Ezquerro and C. Tickle, Development **127**, 4811 (2000).
[43] K. Niederreither, J. Vermot, B. Schuhbaur, P. Chambon, and P. Dolle, Development **129**, 3563 (2002).
[44] M. K. Khokha, D. Hsu, L. J. Brunet, M. S. Dionne, and R. M. Harland, Nat. Genet. **34**, 303 (2003).
[45] A. P. Crick, C. Babbs, J. M. Brown, and G. M. Morriss-Kay, J. Anat. **202**, 21 (2003).
[46] X. Sun, M. Lewandoski, E. N. Meyers, Y.-H. Liu, R. E. Max-

son, Jr., and G. R. Martin, Nat. Genet. **25**, 83 (2000).
[47] S. Bergman, O. Sandler, H. Sberro, S. Shnider, E. Schejter, B.-Z. Shilo, and N. Barkai, PLoS Biol. **5**, 0232 (2007).
[48] J. B. Gurdon and P. Y. Bourillot, Nature (London) **413**, 797 (2001).
[49] A. Casali and G. Struhl, Nature (London) **431**, 76 (2004).
[50] S. Dyson and J. B. Gurdon, Cell **93**, 557 (1998).
[51] M. Kerszberg and J. P. Changeux, Proc. Natl. Acad. Sci. U.S.A. **91**, 5823 (1994).
[52] A. Kicheva, P. Pantazis, T. Bollenbach, Y. Kalaidzidis, T. Bittig, F. Julicher, and M. Gonzalez-Gaitan, Science **315**, 521 (2007).
[53] C. Han, T. Y. Belenkaya, M. Khodoun, M. Tauchi, X. Lin, and X. Lin, Development **131**, 1563 (2004).
[54] Y. Morishita and Y. Iwasa (unpublished).